



Published in final edited form as:

J Am Soc Mass Spectrom. 2015 January ; 26(1): 149–158. doi:10.1007/s13361-014-1010-0.

Multifaceted Investigation of Metabolites During Nitrogen Fixation in *Medicago* via High Resolution MALDI-MS Imaging and ESI-MS

Erin Gemperline¹, Dhileepkumar Jayaraman², Junko Maeda², Jean-Michel Ané², and Lingjun Li^{1,3,*}

¹Department of Chemistry, University of Wisconsin - Madison, Madison, WI 53706, USA.

²Department of Agronomy, University of Wisconsin - Madison, Madison, WI 53706, USA.

³School of Pharmacy, University of Wisconsin - Madison, Madison, WI 53705, USA.

Abstract

Legumes have developed the unique ability to establish a symbiotic relationship with soil bacteria known as rhizobia. This interaction results in the formation of root nodules in which rhizobia thrive and reduce atmospheric dinitrogen into plant-usable ammonium through biological nitrogen fixation (BNF). Due to the availability of genetic information for both of the symbiotic partners, the *Medicago truncatula*–*Sinorhizobium meliloti* association is an excellent model for examining the BNF process. Although metabolites are important in this symbiotic association, few studies have investigated the array of metabolites that influence this process. Of these studies, most target only a few specific metabolites, the roles of which are either well known or are part of a well-characterized metabolic pathway. Here, we used a multifaceted mass spectrometric (MS) approach to detect and identify the key metabolites that are present during BNF using the *Medicago truncatula*–*Sinorhizobium meliloti* association as the model system. High mass accuracy and high resolution matrix-assisted laser desorption/ionization (MALDI) and electrospray ionization (ESI) Orbitrap instruments were used in this study and provide complementary results for more in-depth characterization of the nitrogen-fixation process. We used well-characterized plant and bacterial mutants to highlight differences between the metabolites that are present in functional vs. non-functional nodules. Our study highlights the benefits of using a combination of mass spectrometric techniques to detect differences in metabolite composition and the distributions of these metabolites in plant biology.

Keywords

Nitrogen Fixation; *Medicago truncatula*; Metabolites; MALDI; Orbitrap; Mass Spectrometry; Imaging; Q-Exactive

*Address reprint requests to: Lingjun Li, University of Wisconsin at Madison, School of Pharmacy, 5125 Rennebohm Hall, 777 Highland Avenue, Madison, Wisconsin 53705-2222 lingjun.li@wisc.edu Phone: 608-265-8491 Fax: 608-262-5345.

INTRODUCTION

The importance of nitrogen in sustaining life across kingdoms cannot be overstated, as nitrogen is a principal component of many essential biomolecules [1, 2]. Despite its abundance, accounting for approximately 78% of earth's atmosphere in the form of dinitrogen (N_2), most organisms, including plants, are unable to metabolize nitrogen [1, 2]. The process of converting N_2 into the ammoniacal form (NH_3) is referred to as N_2 fixation and can be accomplished via any of the following processes: (i) biogeochemical processes, (ii) an industrial process called the Haber–Bosch process, and (iii) biological processes, through a select group of microorganisms, termed diazotrophs [1]. The contribution of the biogeochemical process is negligible, with the latter two abovementioned processes accounting for the majority of N_2 fixation [1]. The industrial production of nitrogenous fertilizers by the Haber–Bosch process can fulfill the crop nitrogen requirement but with heavy economic and environmental costs [3]. In fact, this process accounts for 50% of the fossil fuel utilization in agriculture and 1-3% of the annual global fossil fuel usage [2]. Furthermore, the cost of nitrogenous fertilizers has increased significantly due to increasing fossil fuel costs. In addition to the increased cost of production, nitrogen fertilizers have also significant environmental and ecological effects. To state a few, nitrous oxide, which is a decomposition product of nitrogenous fertilizer, is much more active than carbon dioxide as a greenhouse gas [2]. In addition, leaching loss, which accounts for 30–50% of the applied nitrogenous fertilizers, leads to the eutrophication of waterways [2, 4]. Therefore, to sustainably feed the burgeoning population, there is an urgent need to optimize alternative nitrogen sources [2]. A select group of microorganisms possesses an enzyme, nitrogenase, which enables them to fix atmospheric N_2 into the ammoniacal form [5]. This process is termed biological nitrogen fixation (BNF), and the amount of nitrogen fixed on land is comparable to that of the Haber–Bosch process [1]. In fact, biological nitrogen fixation was the only major source of nitrogen fixation before the advent of chemical fertilizers and can be performed by either free-living microorganisms or those that live in symbiotic association with other organisms [1, 5]. Symbiotic nitrogen fixation accounts for the bulk of BNF [5] and is principally performed by a group of bacteria collectively called rhizobia in association with the *Leguminosae* family of plants (legumes). This family of plants fixes approximately 40–60 million tons of nitrogen per year and plays a pivotal role in food and energy security [2, 6]. *Medicago truncatula* (Medicago), which is a model legume, has been subject to intense study in the past two decades, not only to determine the molecular, genetic, and biochemical aspects of BNF, but also to understand general legume biology [7-12].

Medicago forms a symbiotic association with the bacterium *Sinorhizobium meliloti*. The process is initiated by the exchange of metabolites [13]. Plants secrete isoflavonoids, the perception of which leads to the secretion of the lipochitooligosaccharide Nod factors by rhizobia. A communication channel is thus established between the host plant and the rhizobia, leading to a series of events culminating in the formation of specialized structures called nodules on the roots of the host plant [14]. These nodules provide an ecological niche inside which the bacterial nitrogenase enzyme is protected from free oxygen and the bacteria differentiate into specialized forms, called bacteroids, which fix atmospheric nitrogen [15]. Critical to the success of this interaction is the nutrient exchange between the host plant and

the bacteria, which requires the plant metabolism not only to supply carbon, nitrogen, and other nutrients to the bacteroids, but also to utilize the metabolites that are released by the bacteroids [6, 15, 16]. Despite the importance of metabolites in this symbiotic association, little work has been done to investigate the array of metabolites influencing this association. Most available studies target a few specific metabolites, the roles of which are either well known or are a part of a well-characterized metabolic pathway [17]. Although recent refinements in various chromatographic and mass spectrometric platforms have led to large-scale, non-targeted metabolic studies in the legume–rhizobium symbiosis, these studies were performed using either homogenized metabolite extracts or *Medicago* cell suspension cultures and fail to provide the spatial distribution of metabolites [17–23].

In the past decade, mass spectrometric imaging (MSI) has rapidly expanded into the field of plant metabolomics as it provides important spatial information about many different molecular species of interest in a single experiment [24–28]. In order to better understand the spatial distribution of metabolites during this symbiosis, we previously used matrix-assisted laser desorption/ionization (MALDI)-TOF MSI on *Medicago* root nodules, identifying amino acids, sugars, organic acids, lipids, flavonoids and their conjugates and demonstrating their distribution in root and nodule tissues [27].

Although it does not provide spatial information, electrospray ionization (ESI)-liquid chromatography (LC)-MS provides complementary results to MALDI-MS due to the different ionization mechanisms of these two techniques. These complementary techniques therefore offer a more complete description of the metabolome that would be critical for a mechanistic understanding of the metabolic exchange that defines nitrogen fixation. Here, we use high resolution MALDI-MSI and ESI-LC-MS for a more in-depth study of the *Medicago* root and nodule metabolomes during nitrogen fixation. In this study, wild-type (wt) plants and rhizobia that are capable of BNF were compared to well-characterized plant and bacterial mutants that are defective in nitrogen fixation in order to detect metabolic differences that are relevant to nitrogen fixation, generating valuable information for understanding the underlying mechanisms of the BNF process.

MATERIALS AND METHODS

Plant Growth and Inoculation with Rhizobia

Medicago seeds were germinated as previously described [29], after which one-day-old seedlings were grown in a growth-chamber on modified Fåhræus medium that was overlaid with germination paper. After 7 days, the roots were inoculated with a rhizobial suspension at $OD_{600} = 0.01$ and grown for 2 weeks. After 14 days, nodules from each sample were selected for metabolite imaging. The plants that were used in this study were *Medicago truncatula* (*Medicago*) Jemalong A17 (wt) and the mutant *dnf1-1*. The bacteria that were used for the inoculation were *Sinorhizobium meliloti* Rm1021(wt) and the mutant VO2683 (*fixJ2.3:Tn5-233*) [30]. The four plant-rhizobia sample combination types that were used in this study are referred to as wt-wt, wt-*fixJ*, *dnf1*-wt, and *dnf1*-*fixJ*.

Tissue Extraction

Root nodules with approximately 1-2 mm of root on each side were detached from the plant, placed into a pre-chilled mortar, flash-frozen with liquid nitrogen and ground to powder. The powder was transferred to a pre-chilled 1.5-mL Eppendorf tube. The metabolites were extracted with 2:2:1 methanol:chloroform:water (v/v). The solution was vortexed briefly and sonicated for 10 min followed by incubation at -20°C for 15 min. The solution was then centrifuged at $20,000 \times g$ for 10 min to pellet the plant material. The resulting aqueous supernatant was collected and dried in a SpeedVac. The lower organic layer was removed from the plant particulate matter and dried in a SpeedVac. This process was used for all four of the sample types. The samples were stored at -80°C until analysis.

Sample Preparation for MALDI

Root nodules with approximately 1-2 mm of root on each side were detached from the plant. The individual nodules were embedded in gelatin (100 mg/mL in double-distilled water) and gently frozen on dry ice. The frozen tissue was then sectioned into 16- μm slices using a cryostat at -20°C . The sections were thaw-mounted onto a standard glass microscope slide. Matrix (40 mg/mL DHB in 50:50 water:methanol) was applied using a TM Sprayer (HTX Technologies, LLC, Carrboro, NC, USA). DHB was purchased from Sigma-Aldrich (St. Louis, MO, USA).

MALDI-Orbitrap MSI and MS/MS

A MALDI-Orbitrap mass spectrometer (Thermo Scientific, Waltham, MA, USA) that was equipped with an N_2 laser (spot diameter of $75 \mu\text{m}$) was used in positive ion mode for imaging and MS/MS. Three technical replicates of three biological replicates were imaged using a mass range of m/z 100-900, a mass resolution of 60,000, and a mass error of ± 5 ppm. The tissue region to be imaged and the raster step size were controlled using the LTQ Tune software (Thermo Scientific, Waltham, MA, USA). The instrument methods were created using Xcalibur (Thermo Scientific, Waltham, MA, USA). To generate images, the spectra were collected at $75\text{-}\mu\text{m}$ intervals in both the x and y dimensions across the surface of the sample. A list of the detected peaks was automatically created using MSiReader [31] by selecting the wt-wt sample as the “region of interest” and subtracting the peaks from the matrix to create a list of detected m/z values. Ion images were automatically generated from this list using MSiReader. The m/z values that produced ion images in only the wt-wt samples and none of the mutant samples were compiled into a list of “metabolites of interest”. Each metabolite of interest was then manually confirmed as a unique metabolite peak (not an isotope, matrix peak, or artifact) via the manual interpretation of the averaged mass spectrum using ImageQuest (Thermo Scientific, Waltham, MA, USA). MS/MS collision-induced-dissociation (CID) fragments were collected by isolating each m/z of interest and manually adjusting the collision energy for each compound (from 19-42 eV).

Q-Exactive for ESI-MS

To acquire LC-ESI-MS and MS/MS data, four biological replicates of Medicago root nodule extracts were resuspended in either water (for the aqueous samples) or methanol (for the organic samples) to a final concentration of 5 mg/mL. The samples were separated on a

Kinetix C18 column (2.1-mm internal diameter × 150-mm length, 1.7- μ m particle size; Phenomenex, Torrance, CA, USA), equipped with a corresponding guard column, and heated to 35 °C. The mobile phases were (A) water with 0.1% formic acid and (B) acetonitrile with 0.1% formic acid. The aqueous samples were separated within 90 min under the following conditions: 0-10 min, isocratic hold at 1% B; 10-20 min, linear gradient from 1-3% B; 20-68 min, linear gradient from 3-50% B; 68-84 min, linear gradient from 50-95% B; and finally re-equilibration of the system at 1% B for 5 min. The organic samples were separated within 90 min under the following conditions: 0-20 min, linear gradient from 1-50 % B; 20-84 min, linear gradient from 50-99% B; and finally re-equilibration of the system at 1% B for 5 min. The flow rate was 0.3 mL/min and the injection volume was 5 μ L. The samples were kept at 10 °C during the analysis. MS and MS/MS data were acquired on a Q-Exactive instrument (Thermo Scientific, Waltham, MA, USA) that was equipped with an ESI source operated in positive ion mode. The MS scan range was from m/z 75–1000.

The MS/MS scan range was adjusted depending on the parent mass and high-energy collision dissociation (HCD). The MS/MS data were collected for the targeted metabolites at collision energies of 25, 30, 35, and 40 eV. SIEVE (Thermo Scientific, Waltham, MA, USA) was used to determine the “metabolites of interest”. A small molecule component extraction experiment was carried out using SIEVE; the wt-wt samples were used as references and were compared to the 3 mutant samples using 3-5 technical replicates of 4 biological replicates of each sample type. The features were extracted from the data after alignment and framing. The m/z values that had at least 2-fold higher intensity in the wt-wt samples compared to any of the three mutant samples in at least 2 of the biological replicates, a CV <20%, and a p-value < 0.05 were considered “metabolites of interest”. An inclusion list was generated of the “metabolites of interest” and those m/z values were subjected to MS/MS.

Metabolite Identifications

The “metabolites of interest” were identified by searching the accurate mass obtained on the Orbitrap instruments and the MS/MS data using MetFrag [32]. The top 15-20 MS/MS peaks and their intensities were imported into MetFrag, and the neutral exact mass of the parent ion was calculated. The masses were searched within 5 ppm using KEGG, PubChem, and ChemSpider databases. Several adducts were searched for each parent mass, including: [M +H], [M+], [M+Na], and [M+K]. The compounds with MS/MS data that convincingly matched the *in silico* fragmentation, i.e. most or all of the experimental fragment peaks matched theoretical fragments within 10 ppm and no other metabolites in the database matched the experimental fragments, were identified.

RESULTS AND DISCUSSION

MALDI-Orbitrap MS Imaging

This study utilized wild-type (wt) plants and bacteria and the well-characterized plant mutant (*dnf1*) [33, 34] and bacterial mutant (*fixJ*) [27], which are deficient in nitrogen fixation. By comparing the wt-wt samples that are capable of performing nitrogen fixation to

the combinations of mutant samples, wt-fixJ, dnf1-wt, and dnf1-fixJ, which are all incapable of nitrogen fixation, the metabolites that might be relevant to nitrogen fixation were identified. To detect and identify the metabolites that might be relevant to biological nitrogen fixation, MALDI-MSI was performed on Medicago sections from all four of the sample types. Once the data were collected, ion images were generated using MSiReader as described above. The images were manually confirmed as belonging to metabolite peaks, and a list of “metabolites of interest” was generated from the m/z values that produced ion distributions in the wt-wt (functional) nodules but not in any of the three mutant (non-functional) nodules. The representative metabolites that showed distinct distribution patterns in the wt-wt samples and not in the mutant samples are shown in **Figure 1**. **Figure 1a** shows a photograph of each of the four sample types that were used in this study. **Figure 1b** shows the optical image of the four sample types immediately prior to MSI acquisition. **Figure 1c** shows ten representative ion images of metabolites that were found only in the wt-wt samples. These representative metabolites show different spatial distributions throughout the root and nodule portions of the sample, providing further information about these metabolites and their role in nitrogen fixation. **Table S1** in the supplemental information provides a complete list of the “metabolites of interest” that were determined by MALDI-MSI. The MALDI-Orbitrap provides significant advantages for untargeted metabolomics studies compared to more common instrumentation with modest mass spectral resolution, such as MALDI-ToF-ToF instruments, because accurate mass measurements can be acquired, which are essential for metabolomics. Many studies using MALDI-ToF-ToF instruments require accurate masses to be acquired using other instrumentation, typically ESI instruments. This criterion not only increases the number of experiments that need to be performed, but also provides no guarantee that the molecular species of interest that are detected by MALDI will also ionize with ESI. The high resolving power of MALDI-Orbitrap also permits the detection of metabolites that are separated by as little as 0.003 Da. The use of the high mass accuracy and high resolution MALDI-Orbitrap allows for better detection and more complete coverage of the metabolome, which can lead to greater insight into biological processes.

ESI-Q-Exactive MS

To complement the MALDI-MS data, the root nodule extracts of each of the four sample types were also analyzed by LC-ESI-MS using a Q-Exactive instrument. SIEVE software was used to align and frame the replicates of the four sample types, and a list of “metabolites of interest” was compiled for further targeted MS/MS studies using the parameters that were described in the Materials and Methods section. Representative data from SIEVE that were used to select the “metabolites of interest” are provided in **Figure 2**. The panels on the left show XIC (extracted ion chromatogram) peaks, demonstrating that the metabolite has an at least 2-fold greater intensity in the wt-wt samples (blue) compared to any of the mutant samples (red, green, and yellow). The panels on the right display the information on the left in bar graph form, in which each bar represents a different replicate. **Table S2** in the supplemental information provides a complete list of the “metabolites of interest” that were determined by ESI-MS. The ESI experiments produced fewer “metabolites of interest” compared to the MALDI experiments. It is likely that the statistical method of determining the “metabolites of interest” using SIEVE was much more stringent compared to manually

generating a list of “metabolites of interest” using the MALDI data, resulting in fewer metabolite hits. In addition, MALDI tends to ionize a higher number of compounds to begin with for several reasons. First, MALDI produces in-source fragmentation which could fragment delicate molecules into multiple fragments that are then detected. Second, ESI typically ionizes more polar compounds, where MALDI can ionize a wider range of compounds, potentially resulting in higher detection of “metabolites of interest”. Complementary data were obtained using both MALDI and ESI instrumentation; 90 “metabolites of interest” were detected with MALDI, and 21 “metabolites of interest” were detected with ESI. Of the combined 111 metabolites that were detected using both methods, only 7 “metabolites of interest” were detected using both MALDI and ESI.

Metabolite Identifications

Assigning confident molecular identifications for m/z values is typically the bottleneck for untargeted metabolomics studies. Searching the accurate mass alone using the many metabolomics databases that are available online often results in tens to hundreds of possible identifications. MS/MS experiments were conducted on the selected “metabolites of interest” from both the MALDI and ESI studies, although acceptable MS/MS data could not be collected for all of the metabolites that were detected by MALDI-MSI. MetFrag was used to search the accurate mass and MS/MS data. **Figure 3** presents representative results from MetFrag. The peaks correspond to experimental MS/MS data. The precursor ion is shown in blue. Green indicates experimental peaks that matched to *in silico* fragmentation peaks, and red indicates experimental peaks that did not match to *in silico* fragmentation peaks for the selected metabolite. The spectra in Figure 3 indicate good correlation with the *in silico* fragmentation data. Red peaks could be a result of noise/ background ions or other molecular species/isomers with the same or very similar m/z values that were also selected in the fragmentation window. A list of 34 annotated “metabolites of interest” is shown in **Table 1**. Accurate mass and comparison to theoretical fragmentation allows for annotation of identified peaks. For unambiguous metabolite identification, experimental data should be compared with metabolite standards.

The detected peaks may be higher in the wt-wt samples compared to the samples containing plant or bacterial mutants because the fully functional nodules in the wt-wt samples may require a greater activity of the identified metabolites for efficient nitrogen fixation and/or the export of fixed nitrogen to the plants, in contrast to the *wt-fixJ*, *dnf1-wt*, and *dnf1-fixJ* combinations in which non-functional or non-fixing nodules were formed. The identified metabolites belonged to different classes, including organic acids and amino acids. The possible role of some of these metabolites in legume nodulation has either been established or hypothesized, while for most others, the roles have yet to be ascertained. For instance, asparagine has been implicated in nitrogen cycling between various plant organs, and the fixed nitrogen in indeterminate nodules is exported as asparagine for use by plants through the xylem sap of the plant. Similarly, glutamine is also a nitrogen (amide) exporter from indeterminate nodules for use by the plant [35-37]. In addition glutamine, glutamate, and arginine may act as signals indicating the plant's nitrogen status, which in turn is hypothesized to regulate nodule growth and activity [38-40]. Nitrogen fixation is an energy-expending process, and it is estimated that the plants expend approximately 5–12 grams of

carbon for every gram of nitrogen that is fixed. Therefore, this process is tightly regulated, and it is hypothesized that the above-mentioned amino acids act as internal sensors for the plant nitrogen status [41-43].

Proline betaine (the N-methylated form of proline) belongs to a select group of organic osmolytes called compatible solutes, the accumulation of which enables cells to increase the intracellular osmotic pressure, which in turn protects some macromolecular structures during osmotic stress [44]. In addition to being an osmoprotectant, proline betaine also acts as an energy source, in particular as a carbon and nitrogen source for *Sinorhizobium meliloti* in low-osmolarity environments [45]. The ability of *Sinorhizobium meliloti* to utilize proline betaine as an energy source enables this species to colonize legume roots efficiently and offers a competitive advantage against other soil bacteria that compete for plant carbon sources for colonization. Furthermore, betaines induce nodulation (*nod*) genes in *Sinorhizobium meliloti*. Taken together, proline and/or its N-methylated form may act as an important energy source for bacteria during early stages of symbiotic interaction and also prior to bacteroid differentiation in the infection process [46].

A heme moiety is a critical component of leghemoglobins, which are essential for maintaining microaerobic conditions in the nodule environment. The enzyme nitrogenase contains Fe and Mo protein components, which are incompatible with free oxygen, indicating that nitrogenase can function efficiently only under microaerobic conditions [47]. Leghemoglobin monitors the oxygen level in the cytosol of infected cells and maintains this level at optimum concentrations for the functioning of nitrogenase and also for bacterial respiration.

MSI is a relatively new technique in the field of plant sciences. The combination of the high resolution MALDI and ESI Orbitrap instrumentation provides novel advantages over previous studies of biological processes in plant models. Most previously published MALDI-MSI studies of plant metabolites were done with TOF instruments with potential interference from matrix peaks in the low mass region. Thus, these prior studies often required additional experiments on high mass accuracy instruments, typically ESI instruments, in order to identify detected compounds, with no guarantee that metabolites detected with MALDI would also be detected with ESI. Many plant metabolomics studies employ only LC-MS for analysis; employing both LC-MS and MALDI-MSI in our study allows for different types of metabolites to be detected and identified in addition to obtaining spatial information.

CONCLUSIONS AND FUTURE DIRECTIONS

We demonstrated the benefits of using MALDI and ESI for the complementary detection of metabolites, permitting a more in-depth characterization of the Medicago metabolome and nitrogen-fixation process. High-resolution Orbitrap instruments provide the accurate mass measurements that are necessary for metabolite identification. More than 100 “metabolites of interest” were detected using a combination of these MS approaches, only approximately one-third of which were identified based on accurate mass matching and MS/MS fragmentation. The knowledge gained via the comparison of nitrogen-fixing and non-

nitrogen-fixing nodules can provide insight into the roles of metabolites in symbiotic nitrogen fixation. Future studies can use the information gained in this study to elucidate the metabolic pathways that are responsible for nitrogen fixation.

Supplementary Material

Refer to Web version on PubMed Central for supplementary material.

ACKNOWLEDGEMENTS

This work was supported by funding from the University of Wisconsin Graduate School and the Wisconsin Alumni Research Foundation (WARF), a Romnes Faculty Research Fellowship program to L.L. and a National Science Foundation (NSF) grant to JMA (NSF#0701846). E.G. acknowledges an NSF Graduate Research Fellowship (DGE-1256259). The MALDI-Orbitrap and Q-Exactive instruments were purchased through an NIH shared instrument grant (NCRR S10RR029531).

REFERENCES

- Hoffman BM, Lukoyanov D, Yang ZY, Dean DR, Seefeldt LC. Mechanism of nitrogen fixation by nitrogenase: the next stage. *Chem Rev.* 2014; 114(8):4041–4062. [PubMed: 24467365]
- Ferguson BJ, Indrasumunar A, Hayashi S, Lin MH, Lin YH, Reid DE, Gresshoff PM. Molecular analysis of legume nodule development and autoregulation. *J Integr Plant Biol.* 2010; 52(1):61–76. [PubMed: 20074141]
- Lau W, Fischbach MA, Osbourn A, Sattely ES. Key applications of plant metabolic engineering. *PLoS Biol.* 2014; 12(6):e1001879. [PubMed: 24915445]
- Graham PH, Vance CP. Legumes: Importance and constraints to greater use. *Plant Physiol.* 2003; 131(3):872–877. [PubMed: 12644639]
- Dunn MF. Key roles of microsymbiont amino acid metabolism in rhizobia-legume interactions. *Crit Rev Microbiol.* 2014
- Udvardi M, Poole PS. Transport and metabolism in legume-rhizobia symbioses. *Annu Rev Plant Biol.* 2013; 64:781–805. [PubMed: 23451778]
- Cook D. *Medicago truncatula* - a model in the making! Commentary. *Curr Opin Plant Biol.* 1999; 2(4):301–304. [PubMed: 10459004]
- Benloch R, Navarro C, Beltran JP, Canas LA. Floral development of the model legume *Medicago truncatula*: ontogeny studies as a tool to better characterize homeotic mutations. *Sex Plant Reprod.* 2003; 15(5):231–241.
- Gallardo K, Le Signor C, Vandekerckhove J, Thompson RD, Burstin J. Proteomics of *Medicago truncatula* seed development establishes the time frame of diverse metabolic processes related to reserve accumulation. *Plant Physiol.* 2003; 133(2):664–682. [PubMed: 12972662]
- Wang HL, Chen JH, Wen JQ, Tadege M, Li GM, Liu Y, Mysore KS, Ratet P, Chen RJ. Control of compound leaf development by FLORICAULA/LEAFY ortholog SINGLE LEAFLET1 in *Medicago truncatula*. *Plant Physiol.* 2008; 146(4):1759–1772. [PubMed: 18287485]
- Branca A, Paape TD, Zhou P, Briskine R, Farmer AD, Mudge J, Bharti AK, Woodward JE, May GD, Gentzbittel L, Ben C, Denny R, Sadowsky MJ, Ronfort J, Bataillon T, Young ND, Tiffin P. Whole-genome nucleotide diversity, recombination, and linkage disequilibrium in the model legume *Medicago truncatula*. *PNAS.* 2011; 108(42):E864–E870. [PubMed: 21949378]
- Samac DA, Penuela S, Schnurr JA, Hunt EN, Foster-Hartnett D, Vandenbosch KA, Gantt JS. Expression of coordinately regulated defence response genes and analysis of their role in disease resistance in *Medicago truncatula*. *Mol Plant Pathol.* 2011; 12(8):786–798. [PubMed: 21726379]
- Rasmussen S, Parsons AJ, Jones CS. Metabolomics of forage plants: a review. *Ann Bot.* 2012; 110(6):1281–1290. [PubMed: 22351485]
- Venkateshwaran M, Volkening JD, Sussman MR, Ané JM. Symbiosis and the social network of higher plants. *Curr Opin Plant Biol.* 2013; 16(1):118–127. [PubMed: 23246268]

15. White J, Prell J, James EK, Poole P. Nutrient sharing between symbionts. *Plant Physiol.* 2007; 144(2):604–614. [PubMed: 17556524]
16. Draper J, Rasmussen S, Zubair H. Metabolite analysis and metabolomics in the study of biotrophic interactions between plant and microbes. *Annu Plant Rev.* 2011; 43:25–59.
17. Desbrosses GG, Kopka J, Udvardi MK. *Lotus japonicus* metabolic profiling. Development of gas chromatography-mass spectrometry resources for the study of plant-microbe interactions. *Plant Physiol.* 2005; 137(4):1302–1318. [PubMed: 15749991]
18. Colebatch G, Desbrosses G, Ott T, Krusell L, Montanari O, Kloska S, Kopka J, Udvardi MK. Global changes in transcription orchestrate metabolic differentiation during symbiotic nitrogen fixation in *Lotus japonicus*. *Plant J.* 2004; 39(4):487–512. [PubMed: 15272870]
19. Suzuki H, Reddy MSS, Naoumkina M, Aziz N, May GD, Huhman DV, Sumner LW, Blount JW, Mendes P, Dixon RA. Methyl jasmonate and yeast elicitor induce differential transcriptional and metabolic re-programming in cell suspension cultures of the model legume *Medicago truncatula*. *Planta.* 2005; 220(5):696–707. [PubMed: 15605242]
20. Farag MA, Huhman DV, Lei ZT, Sumner LW. Metabolic profiling and systematic identification of flavonoids and isoflavonoids in roots and cell suspension cultures of *Medicago truncatula* using HPLC-UV-ESI-MS and GC-MS. *Phytochemistry.* 2007; 68(3):342–354. [PubMed: 17156801]
21. Farag MA, Huhman DV, Dixon RA, Sumner LW. Metabolomics reveals novel pathways and differential mechanistic and elicitor-specific responses in phenylpropanoid and isoflavonoid biosynthesis in *Medicago truncatula* cell cultures. *Plant Physiol.* 2008; 146(2):387–402. [PubMed: 18055588]
22. Harada K, Fukusaki E. Profiling of primary metabolite by means of capillary electrophoresis-mass spectrometry and its application for plant science. *Plant Biotech.* 2009; 26(1):47–52.
23. Kueger S, Steinhauser D, Willmitzer L, Giavalisco P. High-resolution plant metabolomics: from mass spectral features to metabolites and from whole-cell analysis to subcellular metabolite distributions. *Plant J.* 2012; 70(1):39–50. [PubMed: 22449042]
24. Lee YJ, Perdian DC, Song ZH, Yeung ES, Nikolau BJ. Use of mass spectrometry for imaging metabolites in plants. *Plant J.* 2012; 70(1):81–95. [PubMed: 22449044]
25. Kaspar S, Peukert M, Svatoš A, Matros A, Mock HP. MALDI-imaging mass spectrometry - An emerging technique in plant biology. *Proteomics.* 2011; 11(9):1840–1850. [PubMed: 21462348]
26. Gemperline E, Li L. MALDI-mass spectrometric imaging for the investigation of metabolites in *Medicago truncatula* root nodules. *J Vis Exp* (85). 2014
27. Ye H, Gemperline E, Venkateshwaran M, Chen R, Delaux PM, Howes-Podoll M, Ane JM, Li L. MALDI mass spectrometry-assisted molecular imaging of metabolites during nitrogen fixation in the *Medicago truncatula-Sinorhizobium meliloti* symbiosis. *Plant J.* 2013; 75(1):130–145. [PubMed: 23551619]
28. Bjarnholt N, Li B, D'Alvise J, Janfelt C. Mass spectrometry imaging of plant metabolites - principles and possibilities. *Nat Prod Rep.* 2014; 31(6):818–837. [PubMed: 24452137]
29. Catoira R, Galera C, de Billy F, Penmetsa R, Journet E, Maillet F, Rosenberg C, Cook D, Gough C, Denarie J. Four genes of *Medicago truncatula* controlling components of a nod factor transduction pathway. *Plant Cell.* 2000; 12(9):1647–1665. [PubMed: 11006338]
30. Oke V, Long SR. Bacteroid formation in the rhizobium-legume symbiosis. *Curr Opin Microbiol.* 1999; 2(6):641–646. [PubMed: 10607628]
31. Robichaud G, Garrard KP, Barry JA, Muddiman DC. MSiReader: an open-source interface to view and analyze high resolving power MS imaging files on Matlab platform. *J Am Soc Mass Spectrom.* 2013; 24(5):718–721. [PubMed: 23536269]
32. Wolf S, Schmidt S, Muller-Hannemann M, Neumann S. In silico fragmentation for computer assisted identification of metabolite mass spectra. *Bmc Bioinformatics.* 2010; 11
33. Mitra RM, Long SR. Plant and bacterial symbiotic mutants define three transcriptionally distinct stages in the development of the *Medicago truncatula/Sinorhizobium meliloti* symbiosis. *Plant Physiol.* 2004; 134(2):595–604. [PubMed: 14739349]
34. Wang D, Griffiths J, Starker C, Fedorova E, Limpens E, Ivanov S, Bisseling T, Long SR. A nodule-specific protein secretory pathway required for nitrogen-fixing symbiosis. *Science.* 2010; 327(5969):1126–1129. [PubMed: 20185723]

35. Sprent JI, James EK. Legume evolution: where do nodules and mycorrhizas fit in? *Plant Physiol.* 2007; 144(2):575–581. [PubMed: 17556520]
36. Sprent, J. Wiley-Blackwell; 2009.
37. Sulieman S, Tran LSP. Asparagine: an amide of particular distinction in the regulation of symbiotic nitrogen fixation of legumes. *Crit Rev Biotechnol.* 2013; 33(3):309–327. [PubMed: 22793647]
38. Schulze J. Source-sink manipulations suggest an N-feedback mechanism for the drop in N-2 fixation during pod-filling in pea and broad bean. *J Plant Physiol.* 2003; 160(5):531–537. [PubMed: 12806782]
39. Fischinger SA, Drevon JJ, Claassen N, Schulze J. Nitrogen from senescing lower leaves of common bean is re-translocated to nodules and might be involved in a N-feedback regulation of nitrogen fixation. *J Plant Physiol.* 2006; 163(10):987–995. [PubMed: 16876908]
40. Sulieman S, Fischinger SA, Gresshoff PM, Schulze J. Asparagine as a major factor in the N-feedback regulation of N-2 fixation in *Medicago truncatula*. *Physiol Plant.* 2010; 140(1):21–31. [PubMed: 20444196]
41. Parsons R, Stanforth A, Raven JA, Sprent JI. Nodule growth and activity may be regulated by a feedback mechanism involving phloem nitrogen. *Plant Cell Environ.* 1993; 16(2):125–136.
42. Touraine, B. Nitrogen acquisition and assimilation in higher plants. Amancio, S.; S. I, editors. Kluwer; The Netherlands: 2004. p. 1-34.
43. Schubert, S. The apoplast of higher plants: compartment of storage, transport and reactions. Sattelmacher, B.; H, WJ., editors. Springer; The Netherlands: 2007. p. 445-454.
44. Boscarì A, Van de Sype G, Le Rudulier D, Mandon K. Overexpression of BetS, a *Sinorhizobium meliloti* high-affinity betaine transporter, in bacteroids from *Medicago sativa* nodules sustains nitrogen fixation during early salt stress adaptation. *Mol Plant-Microbe Interact.* 2006; 19(8):896–903. [PubMed: 16903355]
45. Alloing G, Travers I, Sagot B, Le Rudulier D, Dupont L. Proline betaine uptake in *Sinorhizobium meliloti*: characterization of Prb, an Opp-like ABC transporter regulated by both proline betaine and salinity stress. *J Bacteriol.* 2006; 188(17):6308–6317. [PubMed: 16923898]
46. Luyten E, Vanderleyden J. Survey of genes identified in *Sinorhizobium meliloti* spp., necessary for the development of an efficient symbiosis. *Eur J Soil Biol.* 2000; 36(1):1–26.
47. Appleby CA. Leghemoglobin and rhizobium respiration. *Ann Rev Plant Physiol and Plant Mol Biol.* 1984; 35:443–478.

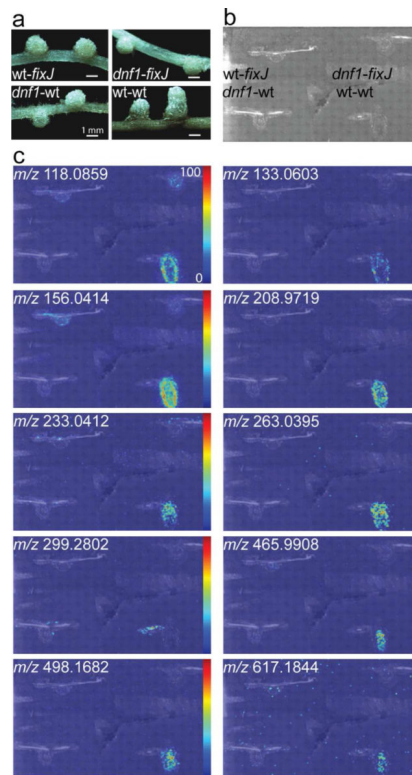


Figure 1. MALDI-MSI of metabolites in Medicago

a) A photograph of all four of the sample types that were used in this study: *wt-fixJ*, *dnf1-fixJ*, *dnf1-wt*, and *wt-wt*. b) Thaw-mounted *Medicago* sections on a glass slide that was covered with DHB matrix prior to MALDI-MSI. c) Representative ion images of metabolites with distinct spatial distributions that were found only in the *wt-wt* samples. Scale bar = 1 mm.

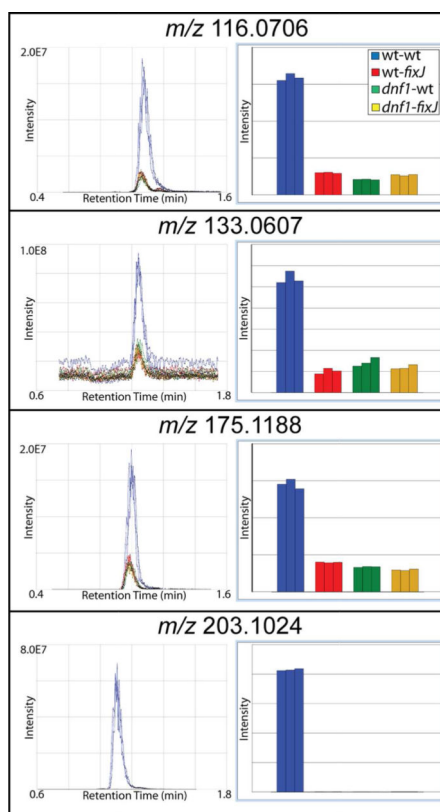


Figure 2. ESI-MS of metabolites in *Medicago*

Representative data from SIEVE, which was used to select the “metabolites of interest”.

Blue indicates wt-wt samples; red indicates wt-*fixJ* samples; green indicates *dnf1*-wt samples; and yellow indicates *dnf1*-*fixJ* samples. The panels on the left show XIC peaks, demonstrating that the metabolite has at least 2-fold greater intensity in the wt-wt samples compared to any of the mutant samples. The panels on the right visualize the information on the left in bar graph form.

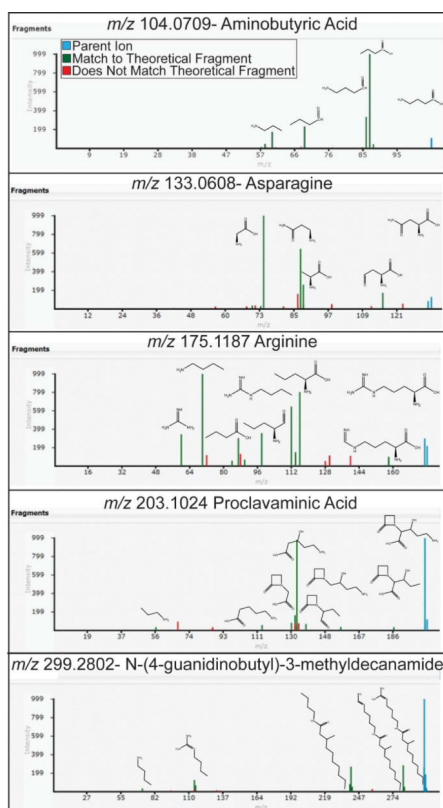


Figure 3. MS/MS data confirmed with MetFrag

Representative MS/MS spectra of the identified “metabolites of interest” and the molecular structures of the matched fragments. Blue indicates the parent ion; green indicates MS/MS peaks that matched the *in silico* fragmentation in MetFrag; and red indicates the experimental peaks that did not match the *in silico* fragmentation.

Table 1

Annotations of “Metabolites of Interest” Detected in Medicigo Root Nodules

Metabolite	Measured <i>m/z</i>	Theoretical <i>m/z</i>	ppm
Aminobutyric acid	104.0708	104.0706	1.9
Methyl-piperidin-iumone [M+]	114.0915	114.0913	1.4
Proline	116.0706	116.0706	0.0
Aminopentene-diol *	118.0863	118.0863	0.0
Isoleucinol	118.1228	118.1226	1.3
Asparagine *	133.0607	133.0608	0.8
Glutamic Acid	148.0603	148.0604	0.9
Asparagine [M+Na] *	155.0425	155.0427	1.3
3-thiophen-1-yl propanoic acid	158.0397	158.0396	0.7
Ethyl-aminocyclopentane carboxylic acid	158.1173	158.1176	1.6
Phenylalanine	166.0859	166.0863	2.1
Asparagine [M+K] *	171.0165	171.0167	1.2
Arginine	175.1187	175.1190	1.4
Tyrosine	182.0810	182.0812	1.0
Methyl-alpha-galactopyranoside	195.0862	195.0863	0.6
Ethyl-aminocyclopentane carboxylic acid [M+K]	196.0731	196.0734	1.7
Proclavaminic acid *	203.1024	203.1026	1.0
Methyl-alpha-galactopyranoside [M+Na] *	217.0678	217.0682	1.8
Proclavaminic acid [M+Na]	225.0840	225.0846	2.4
Proclavaminic acid [M+K]	241.0577	241.0585	3.3
Dihydroxybenzoic acid succinimido ester	252.0500	252.0503	1.2
5-amino-2-(aminomethyl)-6-butoxoxane-3,4-diol [M+Na]	257.1462	257.1472	3.9
9H-fluoren-9-yl-di(propan-2-yl)phosphane	283.1618	283.1610	2.9
N-(4-guamidinobutyl)-3-methyldecamide	299.2802	299.2805	1.1

Metabolite	Measured <i>m/z</i>	Theoretical <i>m/z</i>	ppm
SAM (S-adenosyl-L-methionine)	399.1441	399.1445	1.1
2-hydroxy-5-[[2-phenyl-2-[4-(phenylcarbamoylamino) phenyl]sulfanylacetyl]amino]benzoic acid	514.1423	514.1431	1.5
2-[hydroxy-(2R)-3-hydroxy-2-[(9E,12E)-octadeca-9,12-dienoyl]oxypropoxy]phosphoryl]oxyethyl]-trimethylazanium [M+]	520.3395	520.3398	0.5
Oleoyl lysophosphatidylcholine	522.3552	522.3554	0.5
18-[(4Z)-4-[(2-hydroxy-5-nitrophenyl)hydrazinylidene]-3-oxocyclohexa-1,5-dien-1-yl]octadecanoic acid [M+]	541.3125	541.3146	3.9
3-[[[[[(2R,3S,4R,5R)-5-(6-aminopurin-9-yl)-3,4-dihydroxyoxolan-2-yl]]methoxy-hydroxyphosphoryl]oxy-hydroxyphosphoryl]oxy-hydroxyphosphoryl]oxypropanoic acid	580.0223	580.0242	3.1
[[[(2R,3S,5R)-5-[4-amino-5-(4-aminobutyl)disulfanyl]-2-oxopyrimidin-1-yl]-3-hydroxyoxolan-2-yl]methoxy-hydroxyphosphoryl] phosphono hydrogen phosphate [M+]	602.0052	602.0067	2.4
(Z)-4-oxo-2-[(Z)-1-oxooctadec-9-enyl]-12-henicosenoic acid	603.5340	603.5347	1.1
1,3-dilinolenin	613.4814	613.4827	2.0
Heme	617.1844	617.1846	0.4

Ions are [M+H] unless otherwise specified.

* Found in both MALDI and ESI